

## Suspended timber ground floors: measured heat loss compared with models

S. Pelsmakers , B. Croxford & C.A. Elwell

To cite this article: S. Pelsmakers , B. Croxford & C.A. Elwell (2017): Suspended timber ground floors: measured heat loss compared with models, Building Research & Information, DOI: [10.1080/09613218.2017.1331315](https://doi.org/10.1080/09613218.2017.1331315)

To link to this article: <http://dx.doi.org/10.1080/09613218.2017.1331315>



© 2017 The Author(s). Published by Informa UK Limited, trading as Taylor & Francis Group



Published online: 26 Jun 2017.



Submit your article to this journal [↗](#)



Article views: 770



View related articles [↗](#)



View Crossmark data [↗](#)

## Suspended timber ground floors: measured heat loss compared with models

S. Pelsmakers <sup>a</sup>, B. Croxford <sup>b</sup> and C.A. Elwell <sup>c</sup>

<sup>a</sup>School of Architecture, University of Sheffield, Sheffield, UK; <sup>b</sup>UCL Institute for Environmental Design and Engineering, University College London, London, UK; <sup>c</sup>UCL Energy Institute, University College London, London, UK

### ABSTRACT

There are approximately 6.6 million dwellings in the UK built before 1919, predominantly constructed with suspended timber ground floors whose thermal performance has not been extensively investigated. The results are presented from an *in-situ* heat-flow measuring campaign conducted at 27 locations on a suspended timber ground floor, and the estimated whole-floor *U*-value compared with modelled results. Findings highlight a significant variability in heat flow, with increased heat loss near the external perimeter. *In-situ* measured-point *U*-values ranged from  $0.54 \pm 0.09 \text{ Wm}^{-2} \text{ K}^{-1}$ , when away from the external wall perimeter, to nearly four times as high ( $2.04 \pm 0.21 \text{ Wm}^{-2} \text{ K}^{-1}$ ) when near the perimeter. The results highlight the fact that observing only a few measurements is likely to bias any attempts to derive a whole-floor *U*-value, which was estimated to be  $1.04 \pm 0.12 \text{ Wm}^{-2} \text{ K}^{-1}$  and nearly twice that derived from current models. This raises questions about the validity of using such models in housing stock models to inform retrofit decision-making and space-heating-reduction interventions. If this disparity between models and measurements exists in the wider stock, a reappraisal of the performance of suspended timber ground floors and heat-loss-reduction potential through this element will be required to support the UK's carbon-emission-reduction targets.

### KEYWORDS

housing; performance gap; retrofit; suspended timber ground floors; thermal conductivity; thermal performance; *U*-value

### Introduction

The majority of the UK's 27 million dwellings are not well insulated (DECC, 2012), and most of these will still be in use in 2050 (Killip, 2008; Power, 2008; SDC, 2006), while housing alone is responsible for approximately 30% of the UK's total emissions (DECC, 2011). An estimated 6.6 million dwellings in the UK were constructed before 1919 (Thorpe, 2010), which are predominantly of solid-wall construction (Baker, 2011a; DCLG, 2009; Rock & Macmillan, 2005) and suspended timber floors (Rock & Macmillan, 2005). Including later 1930s' homes, there might be as many as 10 million dwellings with suspended timber ground floors in the UK alone (Dowson, Poole, Harrison, & Susman, 2012).

About 50% of the energy demand in pre-1919 housing is for space heating (DCLG, 2006, 2012; Palmer & Cooper, 2011; Utley & Shorrocks, 2008); the majority of this heat is lost through insufficiently insulated walls and roofs (NEF, 2011), while ground-floor heat loss is estimated to be between 10% and 25% of the total (Harris & Dudek, 1997; NEF, 2011), depending on housing

typology and fabric efficiency standards. Although the UK has committed to reduce CO<sub>2</sub> emissions by at least 80% by 2050 from 1990 levels (HM Government, 2008), it is estimated that only about 4% of solid walls in the UK's pre-1919 properties are insulated (DECC, 2015), and it is unknown how many pre-1919 ground floors are insulated. This may be partly due to a large proportion of pre-1919 housing being expensive, disruptive and difficult to upgrade, and therefore classified as hard to treat (Beaumont, 2007; DCLG, 2012; Dowson et al., 2012; Thorpe, 2010; Wetherhill, Swann and Abbott, 2012). Reducing the significant heat loss from the pre-1919 housing stock clearly presents an opportunity to meet ambitious carbon-reduction targets and improve occupant thermal comfort (Bernier, Ainger, & Fenner, 2010; Lowe, 2007).

A key aspect of the UK's planned transition to a low-carbon economy (DECC, 2009, 2012) is reducing the carbon emissions associated with domestic space heating, which currently account for approximately 13% of the UK's emissions (DECC, 2009). Generally, carbon-

reduction policies and incentives are based on the payback of retrofit interventions (Clinch & Healy, 2001), where the energy savings from interventions give a financial return on the initial investment over time. This payback for retrofit interventions depends on the accurate estimation of the performance of the construction element and on the actual achieved improvement in thermal performance. In support of achieving the targeted energy-use savings and associated carbon-emission reductions, accurate pre- and post-retrofit models are required. However, specifically for the pre-1919 housing stock, inaccurate models were considered to be partly responsible for the recently reported performance gap, *i.e.* disparities between the predicted and the actual performance of existing construction elements (May & Rye, 2012). For example, the models were found to overestimate the  $U$ -values for solid walls in the UK when compared with actual *in-situ* measurements (Baker, 2011b; Birchall, Pearson, & Brown, 2011; Li et al., 2014).

At present, suspended timber ground floors are not well characterized and the lack of *in-situ*  $U$ -value measurements for suspended timber ground floors hinders retrofitting decision-making. For suspended timber ground floors, a recent study suggests that models might underestimate suspended ground-floor heat loss; however, this was based on a thermal chamber study at the Salford Energy House (Pelsmakers et al., 2017). The current paper presents the results of high-resolution *in-situ* measurements of a suspended timber ground floor in a pre-1919 terraced house in west London, UK. This research, based on a single case study house, is unlikely to provide representative numerical results for the entire pre-1919 UK housing population. Therefore, it focuses on the physical insights and qualitative results to highlight trends and methodological implications (Flyvbjerg, 2006) as well as the potential energy and retrofitting policy implications arising from this.

The aim of the study was to investigate whether the thermal chamber findings were also applicable in a real house in the field and specifically: (1) to investigate the expected large variation of heat flow across the floor in a real house; (2) the implications of this for *in-situ* measuring techniques and comparison with models; and (3) to investigate the potential disparity between modelled and measured floor  $U$ -values.

The paper is structured as follows. First, the case study house and research method are discussed, including instrumentation, the *in-situ* measuring method and associated measurement uncertainties. The results, analysis of the results and discussion are then presented, focusing on the variation of heat loss across the floor and comparison between *in-situ* measured and modelled  $U$ -values and on the implications arising from

these findings, *e.g.* *in-situ* measuring techniques and potential policy uncertainty when relying on modelled results.

## Case study house

The case study house was a 1910 solid-wall, two-bedroom terraced house located in the conservation area of the Brentham Estate (Garden Suburb) in Ealing, west London (Figure 1). It was unoccupied during the duration of the 13-day study conducted in January 2014. Its front facade is west facing; the 12.15 m<sup>2</sup> living room floor (44% of the total ground floor area) had bare floorboards with three exposed airbricks located in the void between joists, allowing some airflow movement between floor sections (Figure 2). One airbrick (near sensor location 1) was sheltered by a hedge. On average the living room floor void was 250 mm deep below the 100 mm joists and was divided in four void sections by three sleeper walls (Figure 3). The ground surface of the floor void consisted of up to 150 mm concrete oversite underneath dust and rubble, ascertained from a site survey by drilling into the ground. Case



**Figure 1.** The case study house in the Brentham Estate conservation area, front facade.

*Note:* The wide hedge on the left-hand side is also partially sheltering an airbrick.



**Figure 2.** An airbrick in between the joists.

study floor characteristics are listed in Table 1. Two airbricks on the back facade, below a different room, were partially protected by a greenhouse lean-to structure and services. The living room floor void was isolated from the floor voids elsewhere. Only the living room

floor was monitored due to the location of furniture and fitted kitchen units and access issues (Figure 3). The case study was a terraced house, like just over 50% of pre-1919 houses (Gentry, 2010), with a floor construction similar to others in the Brentham Estate (nearly 700 houses). However, it is not known how prevalent are the sleeper wall locations, nor how common the presence of oversite concrete is in the wider housing stock.

## Instrumentation

Instrumentation was undertaken in accordance with ISO-9869 (unless stated otherwise) and as described below.

### Heat-flux sensors

Hukseflux HFP01 ( $\pm 5\%$  accuracy) heat-flux sensors were placed in accordance with a grid, aligning sensors in both

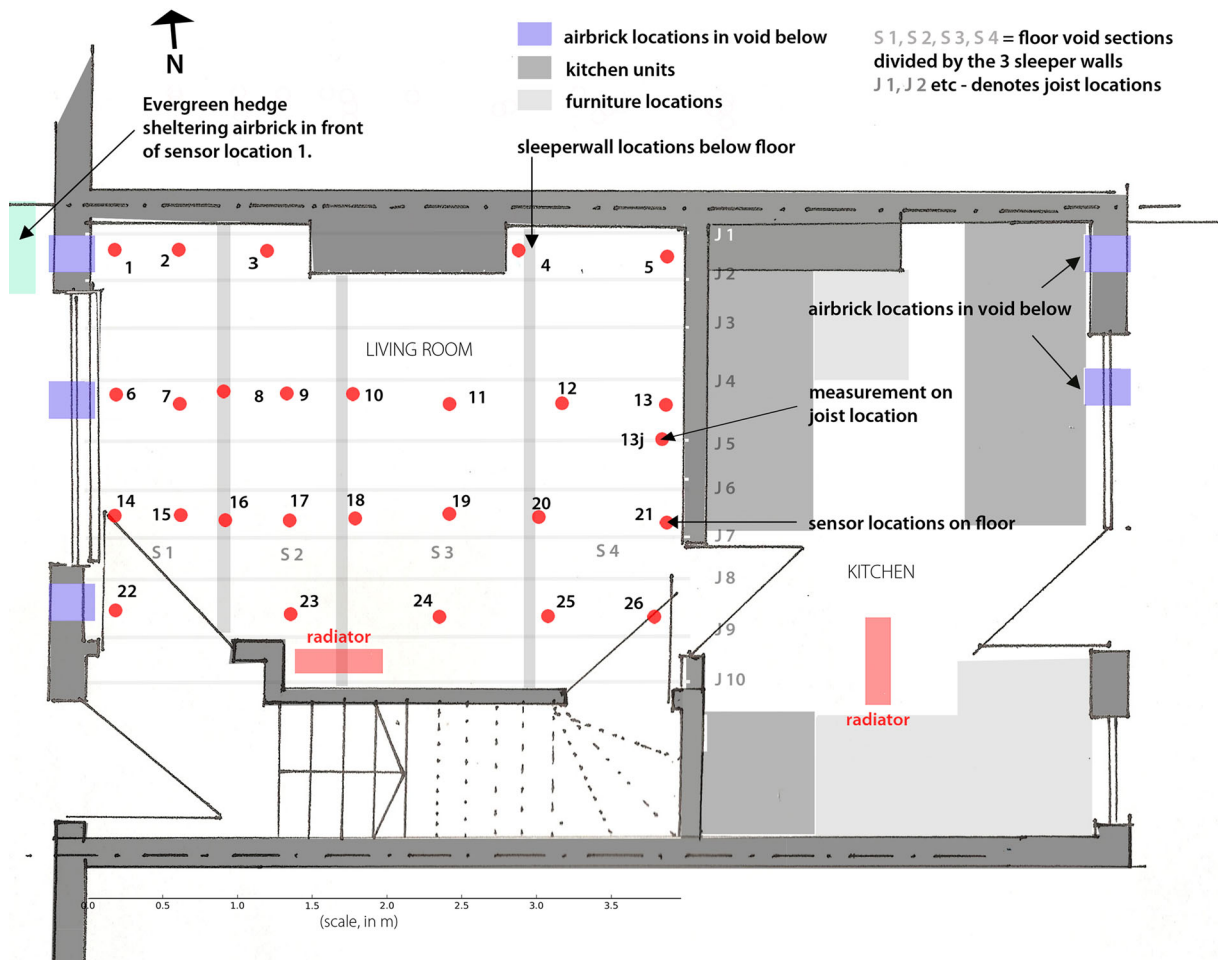


**Figure 3.** Floor plan with heat-flux sensor locations (indicated by circles and numbered); airbrick locations (square boxes); and sleeper walls (grey). Approximate joist locations are marked with a faint grey line and annotated with J1, J2 etc.

Note: Sensor locations 1–5 are in line with the partially sheltered airbrick. Locations 6–13 are located in line with the central airbrick, representing one of two higher-resolution monitoring grids; the second higher-resolution grid includes sensors in locations 14–21, which are not located in line with an airbrick below. Sensor locations 22–26 are located in line with another exposed airbrick, while location 13j is the only location measured on a joist. Portable radiant oil-filled electrical plug-in heaters are marked.

**Table 1.** Case study house characteristics from site survey and typical model assumptions.

Perimeter ( $P$ )	9.1 m (breadth ( $b$ ) = 4.55 m; length 6.1 m)
Total ground floor area ( $A$ )	27.7 m <sup>2</sup>
$P/A$	0.33 m/m <sup>2</sup>
$B^* = A/0.5P$ , where $B^*$ is the characteristic dimension of the floor and is the floor area ( $A$ ) divided by half the exposed floor perimeter ( $P$ )	6.09 m
Airbrick ventilation opening area	0.022 m <sup>2</sup>
Total ventilation opening area per metre of exposed perimeter	0.0024 m <sup>2</sup> /m
Joist dimensions	0.050 × 0.100 m
Joist spacing (centre to centre)	About 0.35–0.39 m c/c
% Joist versus floor board	12%
Floor board thickness (19 mm)	0.019 m
Softwood conductivity ( $k$ , joists and floorboards)	0.13 Wm <sup>-1</sup> K <sup>-1</sup> (Anderson, 2006)
Soil conductivity ( $\lambda_g$ )	100% clay assumed: 1.5 Wm <sup>-1</sup> K <sup>-1</sup> (CIBSE, 2015), under approximately 100 mm over site concrete (conductivity unknown)
Foundation wall thickness ( $d_w$ )	0.22 m (based on a single brick width)
Thermal transmittance of the foundation wall ( $U_w$ )	1.7 Wm <sup>-2</sup> K <sup>-1</sup> (CIBSE, 2015)
Height of the floor surface above the external ground level ( $h_f$ )	On average 0.17 m (to the front 0.270 m and to the back 0.070 m; 0.25 m average void depth below 0.1 m joists)
Internal surface thermal resistance ( $R_{si}$ )	0.17 m <sup>2</sup> KW <sup>-1</sup> (CIBSE, 2015)
External surface thermal resistance ( $R_{se}$ )	0.04 m <sup>2</sup> KW <sup>-1</sup> (CIBSE, 2015)
Average wind speed at 10 m ( $v$ )	Assumed to be 5 m/s based on RdSAP as a top limit
Wind shield factor ( $f_w$ )	Suburban assumed: 0.05 (BSI, 2009)

Note: The ventilation area required per exposed perimeter by Part C of the current English Building Regulations is 0.0015 m<sup>2</sup>/m, which is exceeded in this case.

directions (Figure 3). However, some grid offsets occurred caused by uneven floorboards or the presence of nails or staples (making them unsuitable for sensor fixings). Instead, a nearby suitable sensor location was used. *In-situ* heat-flux sensors were placed in 27 locations on the living room floor (Figure 4): 18 sensors were placed in line with the airbricks below (locations 1–13 and 22–26); and eight sensor locations were offset from airbrick locations (sensors 14–21). The presence of nails to fix floorboards to joists made the joists generally difficult places on which to fix heat flux sensors; only one location was therefore measured on a joist (location 13j in Figure 3).

The active sensing part of the heat-flux sensors (30 mm in the middle of the 80-mm sensor) was kept

**Figure 4.** Instrumentation set-up on the bare floorboard surface of the case-study house.

free from any tape or instruments; sensor placement was undertaken with the use of infrared images and fixed with a thin layer of Servisol heat-sink compound (thermal conductivity = 0.9 Wm<sup>-1</sup> K<sup>-1</sup>; Farnell, 2014) and black duct tape (to best match the dark brown floorboard's colour and emissivity) along the edges and the first 100 mm of the lead. Sensors were connected to Eltek Remote Sensor GENII data loggers or Squirrel 451 L or 851 L data loggers and were downloaded at regular intervals to avoid data loss. Direct solar gain on all instruments was avoided by closing a white reflective window blind at all times. All measurements were taken at five-minute sequential intervals and for  $U$ -value estimation were analysed at daily intervals.

### Temperature sensors

$U$ -values are estimated from 'air to air' environments (BSI, 2014) (which is usually also the model assumption; IEA, 2012; Szokolay, 2008), including for the floor  $U$ -value model (BSI, 2009). While external air temperatures were accordingly used, internal surface temperatures instead of internal air temperatures were used, and accounted for in the analysis with the incorporation of an internal surface resistance. The use of internal surface to external air temperatures is commonplace (e.g. as described by Li et al., 2014; Baker, 2011b; and Rye & Scott, 2012) as interior air temperature sensors are vulnerable to disruption and challenging to locate appropriately with typically highly inhomogeneous temperature profiles within the room. The external air temperature ( $T_{ea}$ ,  $\pm 0.4^\circ\text{C}$  accuracy, protected by a Stephenson screen) was monitored at the front of the house, near the observed floor below the first-floor window, placing the sensor away from any public interference or theft. Uncertainty arising from external temperature sensor location is unknown but is likely included in the

**Table 2.** Identified errors and applicability; after ISO-9869 (BSI, 2014), with replacement of the ISO-9869 'natural variability error' of  $\pm 10\%$  with the standard deviation (SD) of daily  $U$ -values; grouping by authors.

Identified errors (after ISO-9869)	Applicable for each point measurement
Intrinsic: instrument error (calibration heat-flux and temperature sensors)	$\pm 5\%$
Extrinsic: measuring condition error – edge heat-loss error	$\pm 3\%$
Extrinsic: measuring condition error – contact error	$\pm 5\%$
Extrinsic: measuring condition error – temperature location-measurement error	$\pm 5\%$
Natural variability $U$ (inherent property, not a measurement error) – SD of daily $U_{\text{mean}}$	$\pm 5\text{D}$
Final estimated error	$\sqrt{5^2 + 3^2 + 5^2 + 5^2 + \text{SD}^2}$ (equation 3)

Note: The ISO-9869 estimated error is  $\sqrt{5^2 + 3^2 + 5^2 + 5^2 + 10^2} = \pm 14\%$  (BSI, 2014). Replacement of the ISO-9869 'natural variability error' of  $\pm 10\%$  with the SD of daily  $U$ -values.

uncertainty estimate ( $\pm 5\%$  temperature location measurement error) (Table 2) and is the subject of future research. Heat-flux sensors on the floor were monitored with nearby floor-surface thermistors ( $T_{\text{Si}}$ ,  $\pm 0.1^\circ\text{C}$  accuracy) located next to the heat-flux sensors. Over the monitoring period, the mean  $\Delta T$  of all 27 locations was  $8.67 \pm 0.41^\circ\text{C}$ .

### Space-heating strategy

To undertake *in-situ* heat-flux measurements, a sufficient temperature difference between the internal and external environments is needed. This was achieved by the use of radiant oil-filled electrical plug-in heaters. Doing so removed the confounding influence of the presence of uninsulated central heating radiator pipes in the void. In actual occupied houses, heated and unheated periods occur, and this dynamic pattern was simulated for the duration of the study by a daily heating schedule in accordance with the heating patterns set out in the Building Research Establishment Domestic Energy Model (BREDEM) (Anderson et al., 2001), which is the basis for Standard Assessment Procedure (SAP) models used for building regulations compliance and to compare pre- and post-retrofit efficiency savings (Huebner et al., 2014). In BREDEM, the living area is assumed to be heated for a total of nine hours daily to reach  $21^\circ\text{C}$  between 7:00 and 9:00 hours and between 16:00 and 23:00 hours during weekdays (Anderson et al., 2001). Given that occupancy patterns revealed similar heating patterns at weekdays and weekends in English homes (Huebner et al., 2013; Shipworth et al., 2010), this heating pattern was applied in this study including at

weekends.<sup>1</sup> The dynamic effect of both changing external conditions and the dynamic heating pattern on  $U$ -value estimation is captured by the measurement uncertainty and is discussed below.

### Data analysis and error propagation

*In-situ*-point  $U$ -values ( $U_{\text{p}}$ -values) were estimated according to the mean (or mean of ratios) of daily  $U$ -values as per equation (1), including adjustment with surface thermal resistance ( $R_{\text{Si}}$ ) to account for air-flow and radiative effects at the surface because internal surface temperatures were used. The ISO-9869 'Average Method' or the ratio of means (equation 2) is not the same as the mean of ratios (equation 1) as used in this study, though estimated  $U$ -values are usually closely matched. For this study the ISO-9869 estimated  $U_{\text{ISO}}$ -values were within 0–2% from the estimated  $U_{\text{mean}}$ . Use of  $U_{\text{mean}}$  instead of  $U_{\text{ISO}}$  enabled the statistical treatment of random errors, as applied through equation (3).

Mean or mean of ratios:

$$U_{\text{mean}} = \frac{1}{n} \sum_{j=1}^n 1 / \left( \frac{(T_{\text{Sij}} - T_{\text{eaj}})}{q_j} + R_{\text{Si}} \right) \quad (1)$$

ISO-9868 'Average Method' or ratio of means:

$$U_{\text{ISO}} = 1 / \left( \frac{\sum_{j=1}^n (T_{\text{Sij}} - T_{\text{Sej}})}{\sum_{j=1}^n q_j} + R_{\text{Si}} \right) \quad (2)$$

where  $U_{\text{mean}}$  is the final estimated mean *in-situ*  $U_{\text{p}}$ -value ( $\text{Wm}^2 \text{K}^{-1}$ );  $U_{\text{ISO}}$  is the *in-situ* estimated  $U$ -value derived from the ISO-9869 analysis ( $\text{Wm}^2 \text{K}^{-1}$ );  $q$  is the heat-flow rate ( $\text{Wm}^{-2}$ ), which is inferred using each sensor's unique sensitivity (or calibration factor,  $E_{\text{Sen}}$  ( $\text{mVm}^2 \text{W}^{-1}$ ));  $T_{\text{Si}}$  is the surface temperature of the floor in the room;  $T_{\text{ea}}$  is the external air temperature; and  $R_{\text{Si}}$  is the internal surface thermal resistance, taken to be  $0.17 \text{ m}^2 \text{KW}^{-1}$  in accordance with BSI (2007). Index  $j$  identifies individual measurements in the same location over time; and  $n$  is the number of measurements taken sequentially. All estimates presented here include adjustment for the thermal resistance of the heat-flux sensor itself (approximately  $6.25 \times 10^{-3} \text{ m}^2 \text{K W}^{-1}$  (Hukseflux, 2017)).

When measuring *in-situ* heat-flow in buildings subject to environmental conditions, observed heat flows fluctuate depending on dynamic effects such as heated/unheated periods, day/night, and other environmental and seasonal fluctuations such as solar gain, wind, rain and thermal mass of the observed construction element. Both the ISO-9869 data analysis method (equation 2) and equation (1) represent a steady-state analysis of measurements usually undertaken in dynamic field

conditions. These analysis methods aim to negate dynamic effects by averaging values over a long enough monitoring period and by meeting the three test criteria as described in ISO-9869 to ‘give a good estimate of the steady state’ (BSI, 2014). For this study, all ISO-9869 monitoring test criteria were met for all  $U_p$ -values after 12 days of recording, though they were analysed in accordance with equation (1) for the full 13 days of monitoring.<sup>2</sup>  $U_{ISO}$  was based on five-minute data collected, before outlier removal to ensure 24-hour continuous intervals for the ISO-9869 test criteria, which are based on multiples of 24 hours.

The measurement uncertainty for the *in-situ* estimated  $U_p$ -values is estimated from equation (3) (Table 2). For field data, a clear day and night cycle exists and a daily mean is estimated to determine final  $U_p$ -values; estimated uncertainties are based on ISO-9869-quantified measurement errors (Table 2). The natural variability of the  $U_p$ -value over the monitored period is assumed by ISO-9869 as  $\pm 10\%$  and recognizes that measurements are undertaken in dynamic conditions. However, in this study the natural variability was derived from the standard deviation between daily estimated  $U$ -values to capture the dynamic measuring conditions in the specific uncertainty estimates. As expected, due to the complex interaction between heat transfer and heat storage in thermal mass, changing daily external environmental conditions and a dynamic space-heating pattern (as described above), the natural variability of the uninsulated floor  $U_p$ -value (represented by daily standard deviation (SD)) constitutes a relatively large component of the total uncertainty in the field study: daily SD between  $\pm 4\%$  and  $\pm 13\%$ , leading to total measurement uncertainties between  $\pm 10\%$  and  $\pm 16\%$  depending on point location on the floor (Table 3). This is similar to the  $\pm 14\%$  final estimated measurement uncertainty based on ISO-9869 error propagation (BSI, 2014).

### Removal of outliers

A limited number of outliers were caused by researcher influence (such as blower door tests undertaken during the measuring campaign for other research purposes) and were removed using Chauvenet’s criterion (Taylor, 1997), applied to hourly data. For the 27 sensors on the floor, between three and 10 hourly data points were removed by Chauvenet’s criterion, from a total of 312 hourly data points, *i.e.* up to 3%. This process did not significantly alter the estimated mean  $U$ -values (within 1–2% for each point location); generally outlier removal led to a slightly lower  $U$ -value estimation.

**Table 3.** Estimated  $U_p$ -values for the uninsulated floor alongside their estimated absolute and fractional uncertainties (last column).

Location on the floor	Uninsulated floor mean $U$ -value ( $Wm^{-2}K^{-1}$ )	Final fractional error (%)
HF1 (P)	1.74 ± 0.18	11
HF2 (P)	1.62 ± 0.18	11
HF3	1.25 ± 0.14	11
HF4	0.66 ± 0.09	13
HF5	0.54 ± 0.09	16
HF6 (P)	2.04 ± 0.21	10
HF7 (P)	1.62 ± 0.19	12
HF8 (P)	1.37 ± 0.16	12
<i>HF9</i>	<i>1.11 ± 0.14</i>	13
<i>HF10</i>	<i>0.99 ± 0.13</i>	13
HF11	0.78 ± 0.10	13
HF12	0.69 ± 0.09	14
HF13	0.60 ± 0.09	15
<i>HF14 (P)</i>	<i>1.14 ± 0.12</i>	11
HF15 (P)	1.21 ± 0.12	10
<i>HF16 (P)</i>	<i>1.13 ± 0.11</i>	10
<i>HF17</i>	<i>0.99 ± 0.11</i>	11
<i>HF18</i>	<i>1.01 ± 0.11</i>	11
HF19	0.90 ± 0.11	12
HF20	0.80 ± 0.09	12
HF21	0.60 ± 0.09	15
HF22 (P)	1.99 ± 0.21	11
HF23	1.21 ± 0.14	11
<i>HF24</i>	<i>0.96 ± 0.11</i>	12
HF25	0.75 ± 0.10	13
HF26	0.66 ± 0.10	15
HF_Joist (13j)	0.51 ± 0.07	14

Note: (P) = sensor location was within a 1-m perimeter zone. The seven  $U_p$ -values shown in italics were within the error margins of the estimated whole-floor  $U$ -value.

## Analysis, results and discussion

### Spread of point $U$ -values and the perimeter effect

$U_p$ -values (Table 3) were estimated between  $0.54 \pm 0.09 Wm^{-2}K^{-1}$  (location 5, away from the perimeter) and nearly four times as high in locations 1, 6 and 22 above the airbricks along the perimeter ( $1.74 \pm 0.18$ ,  $2.04 \pm 0.21$  and  $1.99 \pm 0.21 Wm^{-2}K^{-1}$  respectively). The  $U_p$ -value in location 1 may be reduced, compared with the other perimeter locations, by reduced ventilation associated with the airbrick being partially sheltered by a large hedge in that location (Figure 1); the estimated  $U$ -value is in any case within the margins of error of locations 6 and 22 near the exposed airbricks.

As expected, and as also reported for the floor of a thermal chamber (Pelsmakers et al., 2017), a large spread of  $U_p$ -values was observed across the floor in this case

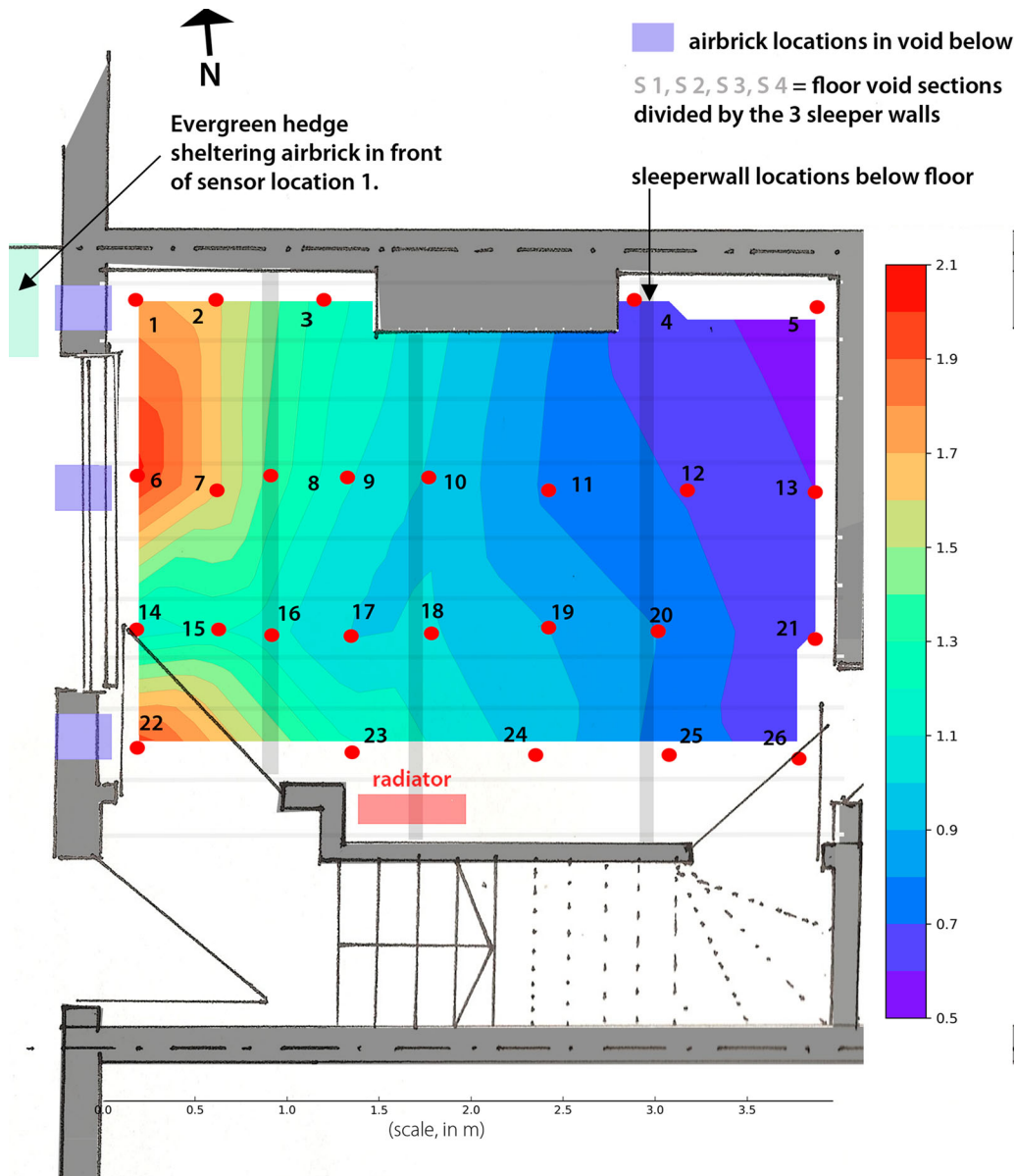


**Figure 5.** Linearly interpolated  $U_p$ -values as a heat map between observed point  $U$ -value locations for the uninsulated floor; point locations are marked with a circle; sleeper wall locations are indicated in light grey shade.

*Note:* Only shown are interpolated values between points, no values between the walls and the points (hence the white zone). For estimated point  $U$ -values, see also Table 3. Joist presence is not accounted for.

study in the field. In general, a clear negative association exists between the measured  $U_p$ -value in a location and its distance from the external perimeter wall: estimated  $U_p$ -values progressively reduce with the distance from the perimeter wall (Figures 5 and 6). This is caused by an increase in the thermal resistance as the distance to the exterior wall increases, while void ventilative heat flow is also lower further away from the perimeter wall airbricks and behind several sleeper wall obstructions (Pelsmakers et al., 2017).

A simplified categorization of a 1 m perimeter zone was used to investigate separately estimated  $U_p$ -values

in non-perimeter and perimeter zones, similarly to Del-sante (1989). As described above,  $U_p$ -values were higher in the perimeter zone for the suspended timber floor and this was supported by an unpaired Mann–Whitney U (Wilcoxon rank sum): Mann–Whitney  $W = 147$ ,  $n_1 = 9$ ;  $n_2 = 17$ ,  $p < 0.05$  (0.00002 or about two tests in 100,000, unpaired), *i.e.* the difference in  $U_p$ -values between the perimeter zone (locations within 1 m from an external wall) and the non-perimeter zone of the floor (sensor locations further away than 1 m) was statistically significant. The estimated mean of the nine perimeter-located point  $U$ -values was  $1.54 \pm 0.17 \text{ Wm}^{-2} \text{ K}^{-1}$ , 1.8 times

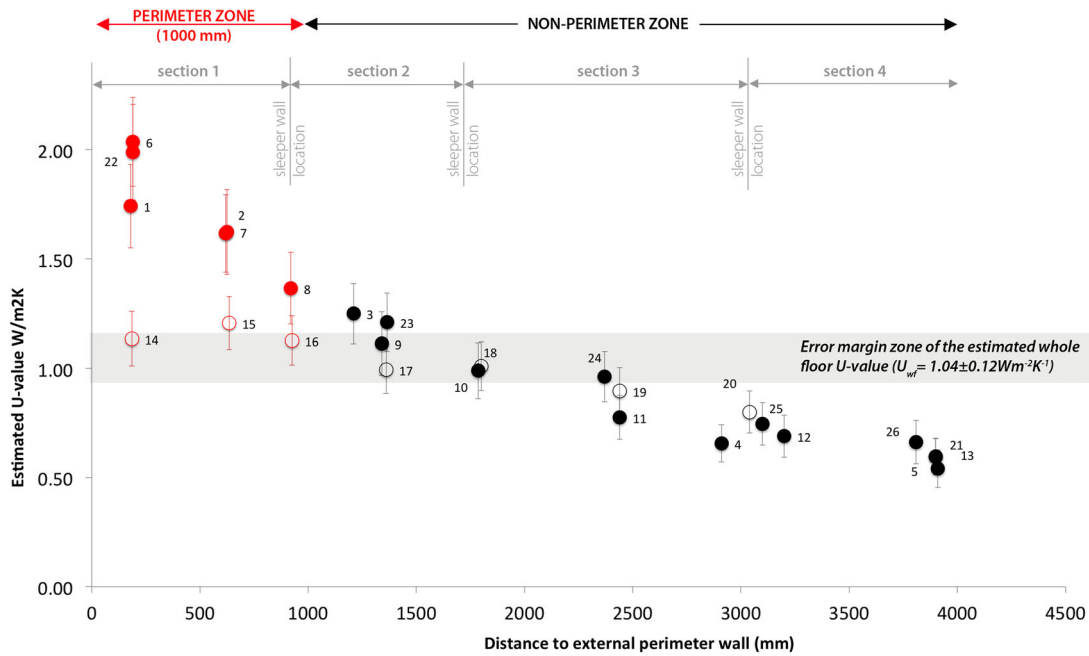


**Figure 6.** The 26 estimated point  $U$ -values on the floor (excluding joist location) presented as a function of the distance to the external perimeter wall; the red data points were located in a 1-m perimeter zone; the black data points were not located in the perimeter zone. The outlined data points are those not aligned with an airbrick below; while the solid ones are aligned with airbricks below.

Note: Error margins were derived as per equation (3). The three sleeper wall locations are marked up, dividing the floor void into four sections. It is unclear why the estimated  $U_p$ -value in location 14 near the perimeter wall was slightly lower than  $U_p$ -values in locations 15 and 16 (further away from the perimeter wall), though values are within estimated error margins. The grey shaded zone denotes the estimated error margin around the whole-floor  $U$ -value.

greater than the estimated mean of the 17 point  $U$ -values located in the non-perimeter zone ( $0.85 \pm 0.11 \text{ Wm}^{-2} \text{ K}^{-1}$ ). Figure 6 shows that there is no abrupt change after 1 m, but instead a gradual reduction in  $U_p$ -values as the distance to the external environment increases (Pelsmakers et al., 2017). It also highlights that when locations were observed in the perimeter zone but not aligned with airbricks in the void below (locations 14–16),  $U_p$ -values were significantly lower than those in front of airbricks (locations 1, 2, 6–8 and 22) and generally these  $U_p$ -values were outside the estimated error margins. However, similar  $U_p$ -values (all within the margins of error) were observed when monitored locations were further away from the perimeter ( $>1$  m distance). This suggests that – in this case study – the effect of the airbricks and void airflow on estimated  $U_p$ -values was no longer clearly visible further away from the 1 m perimeter zone and beyond the first sleeper wall. This might be explained due to the first sleeper wall acting as an obstruction to cross-flow movement of incoming colder external air further along in the void, given that this wall was located at about 0.9 m from the external wall in the void, as also marked on Figures 5 and 6. Similar findings were also observed in a thermal chamber study, where the deep joists and joist direction acted as obstructions to void air flow (Pelsmakers et al., 2017).

### Whole-floor $U$ -value: comparison with literature and models

To compare the 26  $U_p$ -values with model predictions (excluding the joist location), a whole-floor  $U$ -value ( $U_{wf}$ ) needs to be obtained. Generally, the larger the number of point measurements, the greater the certainty in deriving a whole element  $U$ -value. This is especially the case for construction elements with a large variation of heat loss across the surface, as has been illustrated for a floor in a thermal chamber (Pelsmakers et al., 2017) and in this paper for a case study floor in the field: clearly a single or a few ‘point’ measurements are unlikely to be representative of the entire floor. The  $U_{wf}$ -value was estimated as an area-weighted summation in accordance with equation (4) and was estimated as  $1.04 \text{ Wm}^{-2} \text{ K}^{-1}$ :

$$U_{wf} = \sum_{j=1}^n \frac{A_j \times U_{pj}}{A_{wf}} \quad (4)$$

where  $U_{wf}$  is the whole-floor  $U$ -value ( $\text{Wm}^{-2} \text{ K}^{-1}$ );  $A_j$  is the representative floor area ( $\text{m}^2$ ) assigned to each  $U$ -value point ( $U_{pj}$ ); and  $A_{wf}$  is the whole floor area ( $\text{m}^2$ ). Index  $j$  identifies individual point locations on the floor measured simultaneously; and  $n$  is the number of point locations observed. Representative areas around sensors were identified via infrared images, helping to divide the floor surface in a grid in accordance with

the location of sensors in these areas. Different area configurations were tested along the perimeter, but this did not lead to any significant differences. Likewise, different configurations for the whole floor (making assumptions about the whole-floor and kitchen floor area heat loss) lead to  $U_{wf}$ -values within the margins of error of the value reported here. The  $U_{wf}$ -value obtained in accordance with equation (4) was slightly below the arithmetic mean of  $1.09 \pm 0.13 \text{ Wm}^{-2} \text{ K}^{-1}$ , but within the estimated error margins.

Only one  $U_p$ -value was estimated on a joist location (HF13j,  $0.51 \pm 0.07 \text{ Wm}^{-2} \text{ K}^{-1}$ ) and this was just 15% below the nearby floorboard  $U_p$ -value (HF13) of  $0.60 \pm 0.09 \text{ Wm}^{-2} \text{ K}^{-1}$  and within the margins of error. This thermal transmittance reduction is significantly less than the 21%  $U$ -value reduction reported for a thermal chamber (Pelsmakers et al., 2017). However, this difference is likely explained by the joists being nearly half the depth in this case study (100 versus 190 mm in the chamber study) and the sensor location in this study was away from the perimeter, while near the perimeter in the thermal chamber study. As can be expected, the addition of an increased thermal resistance (*i.e.* the joist) will have a greater proportional heat-transfer reduction impact where heat flow is higher (*i.e.* along the perimeter). For the reasons above and given that the difference was within the margins of error, no joist adjustment was made to the  $U_{wf}$ -value for this field study. The  $U_{wf}$ -value was derived from the living room floor only, which represented 44% of the entire ground floor. For model comparisons, the same characteristics of the living room floor were used for the entire floor model.

### Increased uncertainty: whole-floor $U$ -value estimation with fewer point measurements

For practical and resource reasons, most measuring campaigns undertake *in-situ* monitoring in only one or a few locations on a construction element (Rye & Scott, 2012; Rhee-Duverne & Baker, 2013; Baker, 2011b). This was also the case for the few published *in-situ* heat loss measuring campaigns of floors (e.g. Baker, 2011a; Stinson, 2012; Currie, Williamson, & Stinson, 2013; Miles-Shenton, Wingfield, Sutton, & Bell, 2011).

It was found that measuring in just one or two point locations would highly likely lead to significant over- or underestimations of the whole-floor  $U$ -value, as previously reported (Pelsmakers et al., 2017). As illustrated in Figure 6 (the grey zone) and Table 3 (in italics), only seven  $U_p$ -values (or 27% of the observed locations) were within the estimated  $U_{wf}$ -value margins of error (HFs 9, 10, 14, 16–18 and 24). Furthermore, if we consider the

$U_p$ -values and their own margins of error, an additional three  $U_p$ -values fall within the estimated  $U_{wf}$ -value margin of error (Figure 6, grey zone).

Similarly, estimating a whole-floor  $U$ -value from the mean of two paired  $U_p$ -values, only 6.5% of these paired estimates fell within the estimated  $U_{wf}$ -value margin of error (*i.e.* between  $0.92$  and  $1.16 \text{ Wm}^{-2} \text{ K}^{-1}$ ). This increased to 30% if the margins of error of these paired mean  $U$ -value estimates are taken into account (Figure 7). For this case study, this means at least 70% of values, estimated by averaging just two point measurements, would under- or overestimate the whole-floor  $U$ -value. This emphasizes the limitations of low-resolution measurements to obtain a whole-floor  $U$ -value. The random selection of measuring locations is highly likely to lead to a poor representation of the whole-floor  $U$ -value due to the large spread of heat flow across the floor surface. These findings were only obtained exactly by measuring at high resolution across the floor.

Usually measurements along the perimeter are undertaken due to measuring practicalities in occupied houses and this clearly would create a bias when using these perimeter measurements to obtain whole-floor  $U$ -values. In this field study, locations near the airbricks and  $< 800$  mm from the perimeter were generally excluded from the paired values to obtain a close whole-floor  $U$ -value. For single-point measurements, locations not

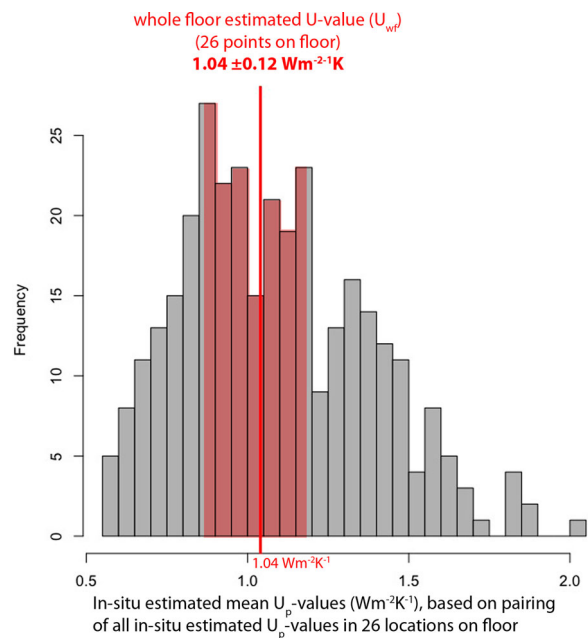


**Figure 7.** Histogram of the 325 paired  $U$ -values.

*Note:* The vertical red line indicates the whole-floor estimated  $U$ -value, while the red (shaded) zone indicates the  $U$ -value distribution within the error margins of the whole-floor  $U$ -value (97 pairs, or 30% of all combinations); the grey bars are mean  $U$ -values from two locations on the floor which, taking into account their own error margins, fall outside the whole-floor  $U$ -value uncertainty margins. No joist presence is accounted for.

aligned with airbricks and up to 2 m away from the perimeter (with two sleeper walls below) were closest to the estimated  $U_{wf}$ -value in this case study.

While the complexity of ground-floor heat-flow mechanisms of this case study is likely typical of the wider housing stock (though not specific detail), there was no prior justification of combining a larger number of  $U_p$ -values to derive an appropriate  $U_{wf}$ -value. Where to measure and the number and combination of  $U_p$ -values requires further research, based on measurements from a number of different case study floors with different characteristics.

### Comparison with other studies

$U$ -values of a ground floor in a terraced house were reported to be between 0.45 and 0.70  $\text{Wm}^{-2} \text{K}^{-1}$ , with a mean of 0.55  $\text{Wm}^{-2} \text{K}^{-1}$ , based on a diversity of literature sources and generally based on model outputs (BRE, 2000; CIBSE, 2015; EST, 2004, 2006, 2007; Griffiths, 2007; SBSA, 2010; Thorpe, 2010). This is clearly significantly below and outside the margins of error of the estimated whole-floor  $U$ -value of  $1.04 \pm 0.12 \text{ Wm}^{-2} \text{K}^{-1}$  (*i.e.* 0.92–1.16  $\text{Wm}^{-2} \text{K}^{-1}$ ) measured for the case study floor presented here.

Only a few *in-situ*-measured studies for floors have been undertaken, and all at low-resolution, making comparison challenging (e.g. Baker, 2011a; Stinson, 2012; Currie et al., 2013; Miles-Shenton et al., 2011). Comparing point  $U$ -values, the estimated *in-situ*  $U_p$ -values located in the perimeter zone in this field study ranged between  $1.14 \pm 0.12$  (location 14) and  $2.04 \pm 0.21 \text{ Wm}^{-2} \text{K}^{-1}$  (location 6), and, when compared with other *in-situ* measurement studies, were similar (though slightly below) the perimeter point  $U$ -values of 1.19–1.93 and 2.4  $\text{Wm}^{-2} \text{K}^{-1}$  as reported by Miles-Shenton et al. (2011) and Stinson (personal communication, 16 August 2012) respectively. However, a comparison of whole-floor  $U$ -values between other *in-situ* sources and the case study reported in this paper cannot be justified because these are *in-situ* point floor measurements from different housing typologies and were generally single-spot measurements in specific locations, unlike the whole-floor  $U$ -value obtained from 26 point locations across the floor in this field study.

### Comparison with modelled $U$ -values

The modelled floor  $U$ -value of the field study house was estimated using several current steady-state floor  $U$ -value models: the ISO-13370 model as described in BSI (2009) as well as the CIBSE (2015), RdSAP (BRE, 2011), but also the superseded CIBSE-1986 model

(CIBSE, 1986). Where possible, input data from the case study site survey were used to inform model inputs to increase the accuracy of the model, as recommended by Park, Norrefeldt, Stratbuecker, Jang, and Grun (2013) and Lee, Lam, Yik, and Chan (2013). Estimates of inputs that could not be obtained from a survey were based on typical assumptions (listed in Table 1). The  $U$ -values were modelled with and without joist presence, but this made no significant difference to the resulting  $U$ -values, given just 12% joist presence (Table 4). The modelled values were within the ranges of reported literature values for terraced houses as described above and, depending on which current model was used, the whole-floor  $U$ -value was estimated to be between 0.51 and 0.57  $\text{Wm}^{-2} \text{K}^{-1}$ , as set out in Table 4. However, in line with findings reported for the Salford Energy House floor (Pelsmakers et al., 2017), these modelled values appeared to underestimate significantly this case study's *in-situ* measured whole-floor  $U$ -value, which was almost twice as high at  $1.04 \pm 0.12 \text{ Wm}^{-2} \text{K}^{-1}$  and outside the estimated margins of error.

When using the superseded CIBSE-1986 model, a floor  $U$ -value estimate of 1.34  $\text{Wm}^{-2} \text{K}^{-1}$  was obtained – overestimating the *in-situ* estimated  $U_{wf}$ -value by almost 30%. While closer to the measured  $U_{wf}$ -value than the current model estimates, this is still outside the margins of error. Possible reasons for the disparity between the old CIBSE-1986 and current floor  $U$ -value models might be associated with a greater influence of ventilation opening area and assumed wind speed in the CIBSE-1986 model. For example, changing default wind speed from 5 m/s (as suggested by RdSAP) to 1 m/s (as recommended by the superseded CIBSE-1986 model) led to the (current) model outputs diverging

**Table 4.** Comparison of the *in-situ*-measured  $U_{wf}$ -value and whole-floor modelled outputs for the field study;  $R_{Si} = 0.17 \text{ m}^2 \text{KW}^{-1}$  used in all models.

Input assumptions as per Table 1, unless stated otherwise (assumed 1 m s <sup>-1</sup> wind speed in parentheses)	Output			Output CIBSE, 1986 (assumed 1 m s <sup>-1</sup> wind speed in parentheses)
	ISO-13370	RdSAP	Output CIBSE	
<i>Estimated U-value outputs (Wm<sup>-2</sup> K<sup>-1</sup>)</i>				
Uninsulated floor, excluding joist presence	0.57 (0.51)	0.51 (0.46)	0.52 (0.45)	1.34 (1.04)
Uninsulated floor, including 12% joist presence	0.57	0.51	0.51	1.31 (1.03)
<i>In-situ measured U-value (Wm<sup>-2</sup> K<sup>-1</sup>)</i>				
$U_{wf}$ estimated from <i>in-situ</i> measurements				1.04 ± 0.12

even further from the *in-situ* measured whole-floor  $U$ -value, whereas the CIBSE-1986 model output reduced to an estimated  $U$ -value of  $1.04 \text{ Wm}^{-2} \text{ K}^{-1}$ , aligning with the *in-situ* estimated whole-floor  $U$ -value for this field study. However, it is unclear whether this result is due to the combination of assumed model input variables for this field study or due to the ability of the CIBSE-1986 model to capture floor thermal transmittance more accurately. A larger sample of high-resolution *in-situ* floor heat-flux measurements of a variety of floors are needed to investigate model accuracy and test whether the CIBSE-1986 model outputs are a better predictor of actual floor thermal transmittance compared with the current models.

The cause of the disparity between the current models and the *in-situ* estimated whole-floor  $U$ -value is unclear and this might be due to a combination of simplified input assumptions (such as wind speed, wind-shielding factors, material and ground conductivity) and model exclusions. For example, wrongful assumptions about ground conductivity can lead to significantly differently estimated  $U$ -values (Harris & Dudek, 1997). Additionally, there might be conceptual differences between modelled and measured, *e.g.* models are simplified, steady-state predictions where thermal mass equilibrium is assumed (BSI, 2009). However *in-situ* measurements in the field are subject to dynamic conditions and practical *in-situ* measuring issues. While dynamic effects are controlled for in the steady-state  $U$ -value analysis and captured in the uncertainty estimates for the monitoring period as undertaken in this study, longer-term seasonal effects outside the monitoring period are excluded; the ability of theoretical models to deal with this level of complexity is yet unknown. Conceptual differences might also relate to the exclusion of linear thermal bridging of the wall–floor junction in floor  $U$ -value models (these effects are to be included in a whole-building model and are excluded in the floor heat-loss model), though *in-situ* measurements were likely affected by the wall–floor junction heat transfer along the perimeter. However, exclusion of the 1 m perimeter values does not fully explain the divergence: a new area-weighted non-perimeter  $U_{\text{wf}}$ -value of  $0.87 \pm 0.11 \text{ Wm}^{-2} \text{ K}^{-1}$  is obtained, which is still 34–41% higher than current model estimates and outside the margins of error of the model, though still within the margins of error of the  $U_{\text{wf}}$  of  $1.04 \pm 0.12 \text{ Wm}^{-2} \text{ K}^{-1}$  when taking the perimeter zone into account. ISO-9869 regards divergences of more than 20% as significant differences (BSI, 2014). Evidently, further research is required to understand which dynamic and steady-state parameters and assumptions create a discrepancy between models and *in-situ* measurements, and how this gap can be bridged

to create more robust models and more informative *in-situ* monitoring.

### **Implications for policy and retrofit decision-making**

Whether the underestimation of modelled  $U$ -values compared with those derived from *in-situ* measurement in this case study is representative of the wider stock is not yet known. Perimeter  $U_{\text{p}}$ -values in this study were similar (though slightly below) those reported elsewhere. However, the absence of a detailed characterization of the thermal performance of suspended timber ground floors in the housing stock, and lack of clear explanation for the discrepancy between measurement and models observed here (and as also reported by Pelsmakers et al., 2017, for a thermal chamber study), raises questions over the validity of policy incentives, payback times and customer satisfaction associated with interventions addressing this building element. If confirmed by further studies in larger samples and covering more floor and housing typologies, such potential differences between modelled and measured  $U$ -value estimates would need to be reflected in policy and retrofit decision-making. For example, if the estimated *in-situ* floor  $U$ -value is significantly greater than assumed and modelled, the benefits of insulating the ground floor might be underestimated, as also noted by Everett, Horton and Duggart (1985) for solid ground-floor heat loss.

The underestimation of the floor  $U$ -value, as reported in this case study, discourages the insulation of floors and focuses attention first on other fabric interventions. If the thermal transmittance and the benefit from insulating floors are underestimated (especially given the disruption to insulate these floors; Killip, 2011) then they might never be insulated and would thus contribute to a performance gap in whole house interventions. Lack of clear empirical characterization of current floor  $U$ -value models, including ISO-13370 on which (Rd)SAP is based and which is used in the UK for regulatory approval, policy and funding decision-making, may also lead to significant errors in the results from housing stock models on which UK national policies are based. As there are millions of uninsulated floors, scaling-up the potentially inaccurately estimated floor heat loss obtained from current models could lead to significant erroneous estimations of energy and associated carbon-emission reductions across the entire existing housing stock. Indeed, alignment of predicted versus actual thermal performance is crucial for stock models and energy-reduction scenarios, as illustrated by Li et al. (2014) for solid walls.

## Conclusions

Suspended timber floors are the ground-floor construction in up to as many as 10 million UK homes, yet their performance is not well characterized. This research undertook unique high-resolution floor  $U$ -value measurements in a case-study house in the field, monitoring 27 locations on a floor; 12–13 days were sufficient for the determination of uninsulated floor  $U$ -values in this study. Findings highlighted the value of high-resolution monitoring techniques compared with the low-resolution measurements usually undertaken. The high-resolution monitoring approach in this study illustrated a clear increased heat loss along the external perimeter wall and reduced heat loss further away from the exposed environment. As expected, this led to a wide variation of  $U_p$ -values across the observed floor: values ranged from  $0.54 \pm 0.09 \text{ Wm}^{-2} \text{ K}^{-1}$  away from the external wall perimeter to values nearly four times as high ( $2.04 \pm 0.21 \text{ Wm}^{-2} \text{ K}^{-1}$ ) along the perimeter. High-resolution monitoring also highlighted that the presence of sleeper walls might act as obstructions to the cross-flow movement of incoming colder external air further along in the void.

The wide spread of  $U_p$ -values also emphasized that estimating  $U$ -values for suspended timber ground floors from low-resolution measurements, which is usually undertaken in practice, often does not produce representative values for the whole-floor  $U$ -value. For example, in this case study, only about 30% of single or paired  $U_p$ -values would give a whole-floor *in-situ* estimated  $U$ -value ( $U_{wf}$ ) within the margins of error of the floor's estimated  $U_{wf}$ -value, highlighting the potential impact of heat-flux sensor locations on  $U$ -value estimation and the potential for bias in  $U_{wf}$ -value estimation from just a few point measurements.

Current literature and models report that the heat loss in suspended ground floors is low. However, the findings in this paper suggest that there might be a disparity between modelled  $U$ -values and those reported in the literature compared with the *in-situ* measured value for this field study. Specifically, this research found that the actual floor heat loss ( $U_{wf} = 1.04 \pm 0.12 \text{ Wm}^{-2} \text{ K}^{-1}$ ), might be significantly underestimated and could be nearly twice as much than previously assumed, though the superseded CIBSE-1986 model gave closer estimates for this case study.

If actual floor heat loss is underestimated, then the benefits from upgrading such floors is also underestimated: there is a greater potential to reduce energy and associated carbon emissions than expected. Given the large number of properties with suspended timber ground floors, erroneous assumptions might have a potentially

significant impact on building stock model outputs, which are used to inform carbon reduction policy and to consequent funding for carbon-reduction measures.

The potential performance gap identified in this field study and the general lack of characterization of the thermal performance of suspended timber ground floors raises questions about the validity of policy incentives, housing stock modelling strategies and policies, payback times, and retrofit decision-making of this construction element.

Larger *in-situ* measuring campaigns covering a diversity of housing and floor typologies, including floors with a different number of airbricks and void airflow and void depth, different perimeter-to-floor area ratios and different sleeper wall configurations *etc.* are needed to understand how the findings can be applied to the wider housing stock. Doing so would also support a better understanding of the different floor archetypes and the impact of those characteristics on floor heat loss, which are unknown at present. Additional studies would also help to refine both measuring and analysis techniques to understand the reasons for potential divergence with models.

## Nomenclature

HF1, HF2, ... =	heat-flux sensor locations 1, 2, ...
$q$ =	<i>in-situ</i> measured heat-flow rate ( $\text{Wm}^{-2}$ ).
$R_{Si}$ =	internal surface thermal resistance, taken to be $0.17 \text{ m}^2 \text{ KW}^{-1}$ for downward heat flow through the floors.
$T_{ea}$ =	external air temperature.
$T_{Si}$ =	internal surface temperature.
$U$ =	thermal transmittance or $U$ -value ( $\text{Wm}^{-2} \text{ K}^{-1}$ ).
$U_p$ =	point $U$ -value; used as a generic description of the small area-based <i>in-situ</i> $U$ -value measurement on a certain location on the floor.
$U_{ISO}$ =	$U_p$ -value obtained in accordance with ISO-9869 'Average Method'.
$U_{mean}$ =	estimated <i>in-situ</i> $U$ -value obtained from a mean of ratios of point $U$ -values ( $U_p$ ).
$U_{wf}$ =	<i>in-situ</i> estimated whole-floor $U$ -value derived from several $U_p$ -values.

## Notes

1. The BREDEM assumes a 07:00–23:00 hours heating schedule at weekends; this was not applied in this study.
2. These ISO-9869 tests were undertaken on raw data, without outlier removal to ensure multiples of a full 24 hours and by using the ratio of the mean to calculate  $U$ -values as per ISO-9869 'Average Method'.

## Acknowledgements

The authors are grateful to the homeowner for the use of their study house, and to following individuals for research input, sharing and feedback: Professor David Shipworth (University

College London – UCL), Dr Sam Stamp (UCL), Dr Jez Wingfield (UCL), Virginia Gori (UCL), Dr Federico Calboli and the Energy Savings Trust (EST) for lending of additional heat flux sensors and data-loggers in support of this study.

## Disclosure statement

No potential conflict of interest was reported by the authors.

## Funding

This research was made possible by support from the Engineering and Physical Sciences Research Council (EPSRC) Centre for Doctoral Training in Energy Demand (LoLo) [grant numbers EP/L01517X/1 and EP/H009612/1] while the corresponding author was at University College London (UCL).

## ORCID

S. Pelsmakers  <http://orcid.org/0000-0001-6933-2626>

B. Croxford  <http://orcid.org/0000-0001-5675-4168>

C.A. Elwell  <http://orcid.org/0000-0003-1058-1091>

## References

- Anderson, B. (2006). *Conventions for U-value calculations*. Watford: BRE.
- Anderson, B., Chapman, P. F., Cutland, N. G., Dickson, C. M., Henderson, G., Henderson, J. H., ... Shorrock, L. D. (2001). *BREDEM-12 Model description*. Watford: BRE.
- Baker, P. (2011a). In situ U-value and 'co-heating' test measurements in a traditional house at New Bolsover, Derbyshire. Glasgow Caledonian University.
- Baker, P. (2011b). *Technical paper 10: U-values and traditional buildings. In situ measurements and their comparisons to calculated values*. Edinburgh: Historic Scotland.
- Beaumont, A. (2007). *W07 – Housing regeneration and maintenance – Hard to treat homes in England*. International conference – Sustainable urban areas, Rotterdam, the Netherlands.
- Bernier, P., Ainger, C., & Fenner, R. A. (2010). Assessing the sustainability merits of retrofitting existing homes. *Proceedings of the Institution of Civil Engineers – Engineering Sustainability*, 163, 197–207.
- Birchall, S., Pearson, C., & Brown, R. (2011). Solid Wall Insulation Field Trials – Report Baseline Performance of the Property Sample. London.
- BRE. (2000). Good Practice Guide 294, Refurbishment guidance for solid-walled houses – Ground floors.
- BRE. (2011). *The government's Standard Assessment Procedure for energy rating of dwellings, SAP 2009, incorporating RdSAP 2009*. Watford: BRE.
- BSI. (2007). *Building components and building elements – Thermal resistance and thermal transmittance – Calculation method ISO 6946: 2007*. London: ISO.
- BSI. (2009). *Thermal performance of buildings – Heat transfer via the ground – Calculation methods (ISO 13370:2007)*. Brussels: BSI.
- BSI. (2014). *ISO 9869-1:2014 – Thermal insulation – Building elements – In situ measurement of thermal resistance and thermal transmittance; part 1: Heat flow meter method*. Geneva, Switzerland: BSI.
- CIBSE. (1986). CIBSE guide – Section A3: Thermal properties of building structures. In CIBSE (Eds.), *CIBSE guide*. London, UK: CIBSE.
- CIBSE. (2015). *CIBSE GUIDE A – Environmental design*. Suffolk, UK: CIBSE.
- Clinch, J. P., & Healy, J. D. (2001). Cost-benefit analysis of domestic energy efficiency. *Energy Policy*, 29, 113–124.
- Currie, J., Williamson, J. B., & Stinson, J. (2013). *Technical paper 19: Monitoring thermal upgrades to ten traditional properties*. Edinburgh, Scotland: Historic Scotland/Edinburgh Napier University.
- DCLG. (2006). *Review of sustainability of existing buildings. The energy efficiency of dwellings – Initial analysis*. London: Department for Communities and Local Government.
- DCLG. (2009). *English House Condition Survey 2007 – Annual report*. London: Department for Communities and Local Government.
- DCLG. (2012). *English Housing Survey HOMES 2010*. London: National Statistics.
- DECC. (2009). *Low carbon transition plan*. London: HMRC.
- DECC. (2011). *DUKES – Domestic energy consumption in the UK 2011. Publication URN 11D/808 ed*. London: Department of Energy and Climate Change.
- DECC. (2012). The energy efficiency strategy: The energy-efficiency opportunity in the UK. London.
- DECC. (2015). Domestic Green Deal, Energy Company Obligation and insulation levels in Great Britain, detailed report. London: DECC.
- Delsante, A. E. (1989). Steady-state heat losses from the core and perimeter regions of a slab-on-ground floor. *Building and Environment*, 24, 253–257.
- Dowson, M., Poole, A., Harrison, D., & Susman, G. (2012). Domestic UK retrofit challenge: Barriers, incentives and current performance leading into the Green Deal. *Energy Policy*, 50, 294–305.
- EST. (2004). *CE83 – Energy efficient refurbishment of existing housing*.
- EST. (2006). *CE184 – Practical refurbishment of solid-walled houses*. London: EST.
- EST. (2007). *CE83 – Energy efficient refurbishment of existing housing*. London: EST.
- Everett, R. H. A., Horton, A., & Doggart, J. (1985). *Linford low energy houses – ETSU-S-1025*. Milton Keynes: Energy Research Group, Open University.
- Farnell. (2014). *Servisol heatsink compound – Technical data* [Online]. Retrieved November 11, 2014, from <http://www.farnell.com/datasheets/319602.pdf>
- Flyvbjerg, B. (2006). Five misunderstandings about case-study research. *Qualitative Inquiry*.
- Gentry, M. S. D. S. M. S. A. (2010). English Heritage scoping study final report v1. Unpublished.
- Griffiths, N. (2007). *The eco-house manual – How to carry out environmentally friendly improvements to your home*. Somerset: Yeovil.
- Harris, D. J., & Dudek, S. J. M. (1997). Heat losses from suspended timber floors. Laboratory experiments measuring heat losses through flooring utilizing a variety of insulation and ventilation rates to determine appropriate strategies for

- retrofitting insulation. *Building Research & Information*, 25, 226–233.
- HM Government. (2008). *Climate Change Act 2008: Elizabeth II (chapter 27) 2008*. Norwich: TSO.
- Huebner, G. M., McMichael, M., Shipworth, D., Shipworth, M., Durand-Daubin, M., & Summerfield, A. (2013). Heating patterns in English homes: Comparing results from a national survey against common model assumptions. *Building and Environment*, 70, 298–305.
- Huebner, G. M., McMichael, M., Shipworth, D., Shipworth, M., Durand-Daubin, M., & Summerfield, A. J. (2014). The shape of warmth: Temperature profiles in living rooms. *Building Research & Information*, 43 (2), 185–196.
- Hukseflux. (2017). *HFP01 heat flux plate / heat flux sensor* [Online]. Hukseflux. Retrieved 2017, from [http://www.hukseflux.com/product/hfp01?referrer=/product\\_group/heat-flux-sensors](http://www.hukseflux.com/product/hfp01?referrer=/product_group/heat-flux-sensors)
- IEA. (2012). Annex 58: ST 3. I Common Exercise on Data Analysis. Opaque Wall. First results.
- Killip, G. (2008). Building A Greener Britain – Transforming the UK's Existing Housing Stock. Environmental Change Institute, University of Oxford, A report for the Federation of Master Builders.
- Killip, G. (2011). *Implications of an 80% CO2 emissions reduction target for small and medium-sized enterprises (SMEs) in the UK housing refurbishment industry* (PhD thesis). University of Oxford.
- Lee, P., Lam, P. T. I., Yik, F. W. H., & Chan, E. H. W. (2013). Probabilistic risk assessment of the energy saving shortfall in energy performance contracting projects – A case study. *Energy and Buildings*, 66, 353–363.
- Li, F. G. N., Smith, A. Z. P., Biddulph, P., Hamilton, I. G., Lowe, R., Mavrogianni, A., ... Oreszczyn, T. (2014). Solid-wall U-values: Heat flux measurements compared with standard assumptions. *Building Research & Information*, 43(2), 238–252.
- Lowe, R. (2007). Technical options and strategies for decarbonizing UK housing. *Building Research & Information*, 35, 412–425.
- May, N., & Rye, C. (2012). Responsible retrofit of traditional buildings. *A report on existing research and guidance with recommendations by STBA*.
- Miles-Shenton, D., Wingfield, J., Sutton, R., & Bell, M. (2011). *Final report to Joseph Rowntree Housing Trust project title: Temple Avenue project part 1/2 – Evaluation of design & construction and measurement of fabric performance*. Leeds: Leeds Metropolitan University.
- NEF. (2011). *Save money by adding insulation to your home* [Online]. National Energy Foundation Retrieved April 2017, from <http://www.nef.org.uk/knowledge-hub/view/insulating-your-home>
- Palmer, J., & Cooper, I. (2011). Great Britain's Housing Energy fact file – 2011. DECC.
- Park, S., Norrefeldt, V., Stratbuecker, S., Jang, Y.-S., & Grun, G. (2013). Methodological approach for calibration of building energy performance simulation models applied to a common 'measurement and verification' process. *Bauphysik*, 35, 235–241.
- Pelsmakers, S., Fitton, R., Biddulph, P., Swan, W., Croxford, B., Stamp, S., ... Elwell, C. A. (2017). Heat-flow variability of suspended timber ground floors: Implications for *in-situ* heat-flux measuring. *Energy and Buildings*, 138, 396–405.
- Power, A. (2008). Does demolition or refurbishment of old and inefficient homes help to increase our environmental, social and economic viability? *Energy Policy*, 36, 4487–4501.
- Rhee-Duverne, S., & Baker, P. (2013). Research into the thermal performance of traditional brick walls. London: English Heritage.
- Rock, I. A., & Macmillan, I. R. (2005). *The Victorian house manual. Care and repair for all popular house types*. Somerset: Haynes Publishing.
- Rye, C., & Scott, C. (2012). The SPAB research report 1. U-value report, revised 2012. London: Society for the Protection of Ancient Buildings.
- SBSA. (2010). Scottish building Standards – Section 6. U-values of ground floors and basements.
- SDC. (2006). Stock take: Delivering improvements in existing housing. Sustainable Development Commission. London.
- Shipworth, M., Firth, S. K., Gentry, M. I., Wright, A. J., Shipworth, D. T., & Lomas, K. J. (2010). Central heating thermostat settings and timing: Building demographics. *Building Research & Information*, 38, 50–69.
- Stinson, J. (2012). *Historic Scotland, technical paper 18, U-value and hygrothermal monitoring for Historic Scotland energy pilots – Draft 2012*. Edinburgh: Edinburgh Napier University for Historic Scotland.
- Szokolay, S. V. (2008). *Introduction to architectural science. The basis of sustainable design*. Oxford: Architectural Press.
- Taylor, J. R. (1997). *An introduction to error analysis. The study of uncertainties in physical measurements*. Sausalito, CA: University Science Books.
- Thorpe, D. (2010). *Sustainable home refurbishment*. London: Earthscan.
- Utley, J. I., & Shorrocks, L. D. (2008). Domestic energy fact file 2008. DECC/EST/BRE.
- Wetherhill, M., Swan, W., & Abbott, C. (2012). The influence of UK energy policy on low carbon retrofit in UK housing. School of the Built Environment, University of Salford.